MULTI-MODAL GRAPHENE POLYMER INTERFACE CHARACTERIZATION PLATFORM FOR VAPORIZABLE ELECTRONICS

V. Gund[1], A. Ruyack[1], K. Camera[2], S. Ardanuc[1], C. Ober[2], and A. Lal[1]
[1]*Sonic*MEMS Laboratory, Cornell University, Ithaca, NY, USA
[2]Ober Group, Cornell University, Ithaca, NY, USA

ABSTRACT

Characterization of physical and chemical properties of organic thin films such as polycarbonates is essential for their application-specific design. In this paper, we report a novel micromechanical resonant membrane platform with both graphene resistivity and mass-dependent frequency sensing to measure the thermal response, vaporization, and subsequent mass change of thin-film analytes deposited on top of the membrane. Graphene transferred on silicon nitride (Si_xN_y) is below the analyte thin film, and the graphene resistance changes due to dangling bond interactions between the analyte film and graphene surface. At the same time, the resonance frequency of the analyte film/graphene/Si_xN_y composite membrane changes with variations in temperature, mechanical properties, mass and elasticity of the analyte film. This device provides a bi-modal characterization of the organic thin film, both in the electrical and mechanical domain, which allows one to identify and optimize the organic film formulation. As an example, we demonstrate differentiating formulations of a polymer blend to realize low degradation temperature, which is critical for vaporizable electronics enabling low-power transience.

INTRODUCTION

The design and synthesis of novel polycarbonates using experimental and theoretical techniques find use in various applications. The polycarbonates are used in electronic components for insulation and as dielectrics, for macro and micro tubing, and in niche applications such as polycarbonate lenses and sterile medical storage. In MEMS microfabrication, these polymers are used in photoresists for lithography and as protective films [1]. However, no single application accounts for more than 10% of the commercial market volume for polycarbonates because of the wide variety of properties offered by these materials [2]. More importantly, the capability to modify and tune their physical and chemical properties, specific to the application, with only minor changes in composition makes them extremely versatile.

Small weight-percent (wt%) additives in polymer blends can drastically change their physical and material properties, and alter their response to temperature and pressure. For vaporizable polycarbonates (VPC), exposure to light of various frequencies can also change chemical properties such as surface bonds and their energies. This enables their use as passive sensors with secure physical encoding of material properties for quantitatively recording light flux intensity and temperature changes [3]. Designing polymers for such applications requires optimization of their glass-transition temperature (T_g) and decomposition temperature (T_d). The polymer effect on electrical conductivity of surrounding materials also needs monitoring. To quickly characterize these blends while exploring a large design space for the VPC, it is impractical to synthesize large quantities of these materials. Small quantities also allow efficient use of reagents. Hence, a microscale characterization platform that can enable polymer characterization with high specificity is essential.

The traditional method of measuring thermal-response of analytes is Thermo-Gravimetric Analysis (TGA). Micromechanical TGA devices use resonant vibrating cantilevers, with integrated piezoresistive sensors, for temperature cycling and measuring corresponding mass-change with shifts in resonance frequencies [4]. However, they do not provide information on dynamic surface interactions. Desorption kinetics of thin-film analytes deposited on microhotplate arrays have been studied using mass spectroscopy [5] but do not have mass-sensing capability. Our device is based on a multi-modal sensing approach that can measure mass-loss and surface-interaction changes simultaneously.

DEVICE CONCEPT

For the characterization platform, we use graphene transferred on a Si_xN_y membrane, as shown in Figure 1. The graphene film is patterned to define electrodes for sensing its resistivity and to selectively heat the suspended region for polymer characterization. A PZT plate is attached to drive the structure at its resonance modes [6].

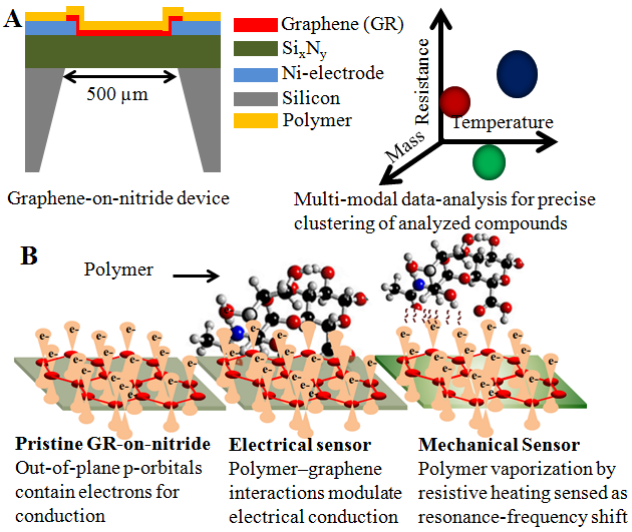

Figure 1: A). Characterization platform with spun-on analyte polymer for thermal cycling B). Polymer surface-interactions with the atomically-thin graphene are sensed electrically with graphene resistivity modulation. The mass-loss and vaporization are sensed mechanically with membrane resonance-frequency shift.

Electrical Sensing

Graphene is an atomically thin sheet of carbon atoms arranged in a honeycomb lattice and shows outstanding electrical properties as a zero-band gap semiconductor with high electrical conductivity [7]. Carbon atoms connected to each other in the lattice are sp^2 hybridized. The remaining p-orbital, with a single electron, is free for conduction. The resistivity of graphene can be, hence, reversibly modulated by molecules adsorbed and desorbed on its surface via charge-transfer. This has been used to study graphene's interactions with a variety of molecules [8] using graphene FETs. Our device measures the modulation of graphene's resistance for sensing surface-modifications during temperature ramp as graphene's atomic interactions with the spun-on polycarbonate change. The graphene also serves the purpose of a resistive heater for temperature ramping with Joule heating.

Mechanical Sensing

The suspended Si_xN_y membrane is the structural layer, actuated at resonance, for mass-sensing in our device. The fundamental resonance frequency of a square membrane, f, in the stress-dominated regime is [9]:

$$f = \frac{1}{a}\sqrt{\frac{\sigma}{2\rho}} = \frac{1}{a}\sqrt{\frac{\sigma V}{2m}} \quad (1)$$

Here, a is the length of the square, σ is the in-built stress and ρ is the density, also expressed as the ratio of mass m to volume V. The second expression yields the relationship for mass-loss Δm to frequency-shift Δf:

$$\frac{\Delta f}{f} = -\frac{\Delta m}{2m} \quad (2)$$

In addition, there is a temperature dependence of the membrane-frequency during heating, based on changes in σ and the membrane dimensions. Since, the membrane is clamped on all sides, and heating is confined to the center of the membrane, the length is constant to first order. However, an effective thermal expansion coefficient (TEC) for the thickness, which can change at the center of the membrane, needs to be accounted for. The temperature dependence, derived from (1), is:

$$\frac{1}{f}\frac{df}{dT} = \frac{1}{2\sigma}\frac{d\sigma}{dT} + \frac{3}{2}\alpha \quad (3)$$

Here, T is the temperature, α is the effective TEC accounting for the Si_xN_y, metal electrodes and spun-on VPC, and t is the thickness of the layers.

The thermal time constant for membrane heating is a few milliseconds due to its small thermal mass. On the other hand, the time to raise the temperature of spun-on VPC and overcome its relatively high heat of vaporization is on the scale of minutes. Hence, during temperature ramp, we expect fast negative shifts in resonance frequency due to membrane heating, a result of effective spring-softening. At sufficiently high input power, we expect this to be followed by a slow positive shift as the VPC heats up and vaporizes, leading to mass-loss.

DEVICE FABRICATION

We have previously demonstrated graphene on Si_xN_y devices for resonator frequency trimming [10]. The fabrication process-flow described therein was used in this work with some modifications. 45 nm thick nickel-electrodes were evaporated and patterned on 360 nm thick Si_xN_y for contact with graphene, which was transferred on top of electrodes. Graphene was also patterned by oxygen plasma-etch only on top of the suspended Si_xN_y to minimize heat losses to the substrate for power-savings.

POLYCARBONATE SYNTHESIS

The polycarbonate used in this study was synthesized based on [3]. VPC was polymerized using the bis(carbonylimidazo1ide) of 2,5-dimethyl-2,5-hexanediol and 80% 1,4- and 20% 1,3-benzenedimethanol. Two different VPC test solutions were made. One consisted of 5 wt% VPC in dichloromethane (DCM) and the other contained 5 wt% VPC + 5wt% (with respect to polymer content) photoacid generator (PAG) (VPC + PAG) in DCM. A PAG, after exposure to ultraviolet (UV) light, provides an acid source, which catalyzes polycarbonates decomposition [11]. By adding PAG to one solution and not the other, we create two different polymer blends with different thermal properties. Each solution was spin coated onto a silicon wafer followed by a post-spin bake of 120 °C for 2 minutes to form a thin film of ~500 nm. The VPC + PAG film was exposed to 254 nm UV light with a dose of 300 mJ/cm^2. Each film was removed from the wafer and the T_d was verified using a commercial TGA. VPC had a T_d of 209 °C, while the VPC + PAG had a lower T_d of 97 °C. After confirmation of different thermal properties, thin films of each blend were spun on graphene devices using the same procedure as above.

TESTING & RESULTS

Unloaded Device - Characterization

Square membranes of side 500 µm were tested for all experiments. Device resonance modes were excited with backside AC PZT actuation and identified with the Polytek MSA 500 laser interferometer. The fundamental mode at 293 kHz with a Q-factor of 1050 in 3 mbar vacuum, shown in Figure 2A, was used. As a control experiment, voltage was ramped across the graphene heater on an unloaded device while simultaneously monitoring membrane resonance frequency shift and graphene resistance change. This is plotted in Figure 2B. With no spun-on polymer, device resonance frequency decreased over millisecond time scales, as expected, due to spring-softening of the membrane with increasing heat. Graphene-resistance varied non-monotonically and approached a value of 8 kΩ at high input-power.

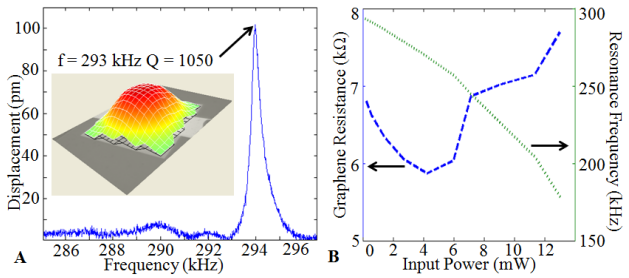

Figure 2: A) Unloaded device fundamental resonance frequency measurement B) Control-measurement of unloaded membrane resonance frequency shift and graphene resistance change vs. input power.

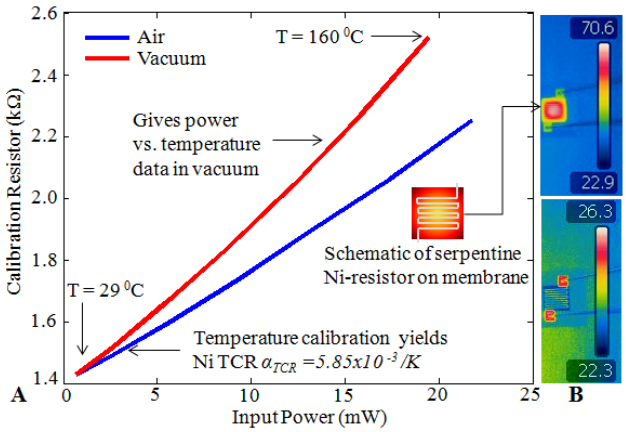

Figure 3: A). Temperature calibration of Si_xN_y membrane devices with serpentine calibration nickel resistors to obtain temperature versus power data in air and vacuum. B). IR camera images of the membrane with calibration resistor, during voltage-ramp in air (blue curve in A)

For temperature calibration, a Si_xN_y membrane with serpentine nickel resistor of baseline resistance 1.46 kΩ at room temperature, and no graphene, was heated by voltage-ramp across the resistor. The membrane surface temperature was monitored with a FLIR T300 infra-red camera while monitoring the nickel resistance, as shown in Figure 3. Using this highly linear calibration data (r^2 = 0.99), the thermal expansion coefficient (TEC) of deposited nickel was extracted as α_{TCR} = 5.85 x 10^{-3}/K with the variation from baseline resistance R_0 given by:

$$R = R_0(1 + \alpha_{TCR}T)$$

The same device was then tested for voltage-ramp in 3 mbar vacuum to obtain a temperature versus power calibration, to account for reduced heat-losses in vacuum.

Polymer-loaded Devices - Resistive Sensing

With spun-on VPC (Device-1) and VPC+PAG (Device-2) polymer, devices were tested with voltage-ramp to heat the polymer while tracking the resonance frequency and graphene resistance. The resistances of the

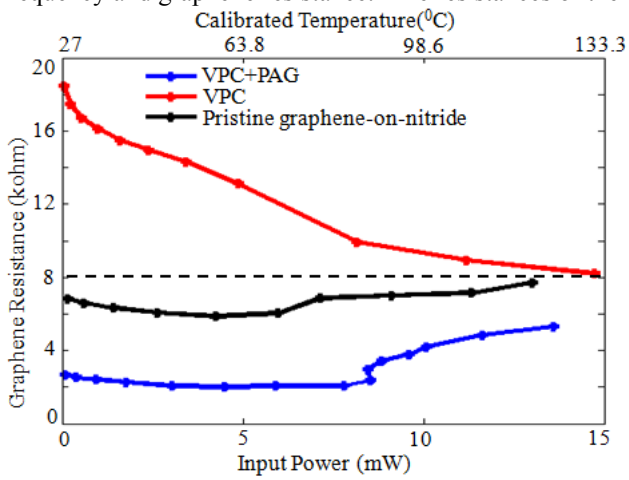

Figure 4: Graphene resistance change due to spun-on polymer, before thermal degradation, varies by 10x between VPC and VPC+PAG. After mass-loss at high input-powers, the graphene is cleaned and both resistances converge to pristine graphene-on-nitride resistance.

graphene on Device-1 and Device-2 before voltage-ramp were 18.6 kΩ and 2.76 kΩ. This indicated high sensitivity of the graphene to small differences in the polymer, in this case the PAG, as a result of different surface interactions. Graphene resistance was modulated with increasing voltage, as VPC degraded thermally. Eventually, as the VPC is "cleaned" off the surface, resistances in both devices approach that of pristine graphene on unloaded devices as shown in Figure 4.

Polymer-loaded Devices - Mass Sensing

The initial resonance frequencies for Devices 1 and 2 were 208.9 kHz and 233.2 kHz respectively. These are lower than the unloaded device frequency of 293 kHz due to different wt% of spun-on polymers. The resonance frequency measured versus time, shown in Figure 5, initially decreased on a scale of milliseconds during steps in voltage-ramp, just like the unloaded devices. However, with higher input-power, the analytes heated up sufficiently and slow-mass degradation was observed on a scale of minutes even as the power was kept constant over those intervals. This measurement is limited by device Q-factor degradation at large input power > 25 mW.

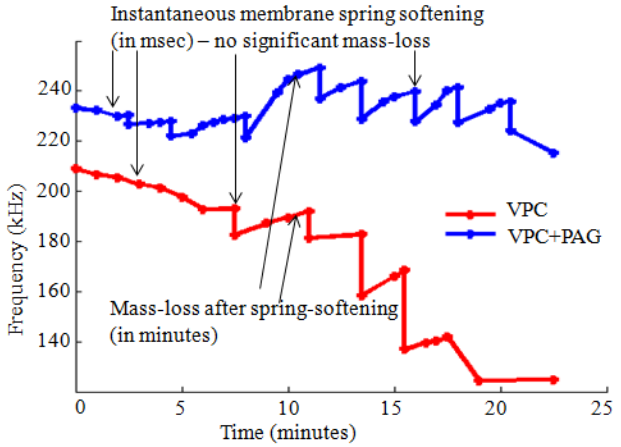

Figure 5: Resonance frequency vs. time during voltage-ramp of the graphene. Regions of only spring softening (low input power), and spring softening followed by mass-degradation (high input power) are shown

To measure mass-degradation versus temperature, the frequency shifts due to spring-softening were subtracted to calculate mass-loss % using (2). This enabled determination of the thermal response of VPCs to increasing input power, and hence, temperature using the calibration data from Figure 3. Simultaneously, the membrane surface was optically monitored with the MSA-500 microscope (20x) to observe VPC vaporization. Figure 6 shows stages in the mass-degradation process mapped to corresponding images of the membrane for Device-2. The measured mass losses for Device-1 and 2 were 33 and 70 % respectively, in reasonable agreement with values of 43 and 60 % obtained by image processing results (using ImageJ software). Residual polymer on the platform, such as in Figure 6D, is due to inefficient heating near the anchors as a result of substrate losses. This can be improved by co-optimization of the electrode design and graphene patterning.

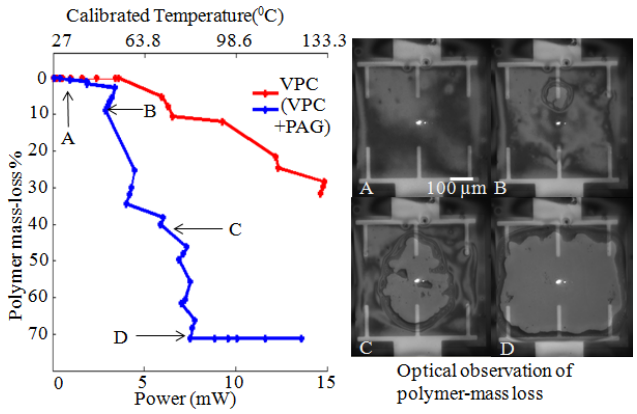

Figure 6: Polymer mass-loss % vs. input power - A) Low input-power with no material loss B) Onset of material loss, also seen optically C) Rapid polymer degradation sensed as a large frequency-shift D) Polymer degradation completed on the membrane. Measured 70 and 33% mass-loss was verified by image processing

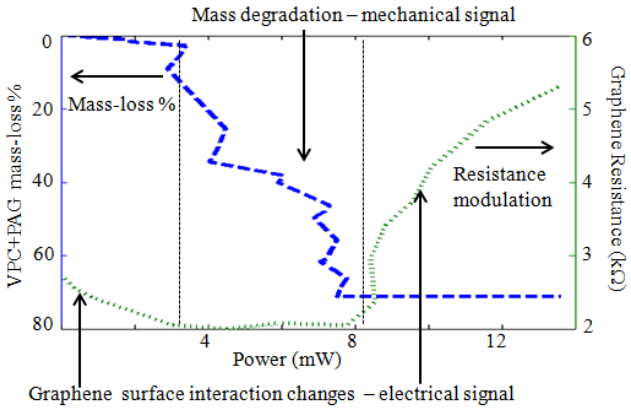

Figure 7: Multi modal polymer characterization - The platform gives complementary electrical and mechanical signals in different input-power regimes, shown by dotted vertical lines, for sensing graphene-polymer surface interactions, mass-degradation, and surface cleaning.

Multi-modal Sensing

By combining frequency and resistance measurements, it is possible to get a 2-dimensional signal for the thermal response of the material, for mass-loss and surface-changes. The signals for Device-2 are shown in Figure 7. The electrical (green curve) and mechanical (blue curve) signals are complementary to each other in this case, highlighting the advantage of sensing with more than one modality. For low input-power, there is almost no mass-degradation producing negligible frequency shifts. However, due to graphene-polymer nanoscale surface interactions, the graphene resistance is modulated significantly. At higher powers, mass-degradation is observed causing large frequency shifts but only small changes in graphene resistance showing minimized surface interactions. At very high powers when mass-degradation is almost complete, no further frequency shifts are seen. However, as the graphene is "cleaned" by high current-drive annealing [12], its resistance approaches that of the unloaded device.

CONCLUSIONS

We have presented a multi-modal characterization platform for polymer analysis using graphene on Si_xN_y as our sensor. While our application is targeted towards VPCs for novel vaporizable electronics, the platform is broadly applicable and can be extended to the analysis of other polymers and spun-on analytes, within the device temperature operation range. As a mW range analysis tool, it is efficient at analyzing picogram quantities of polymers. For thermally degradable polymers, the device can be cleaned by ensuring that the graphene-resistance approaches that of pristine graphene while resonance frequency approaches that of the unloaded device resonance, allowing for cost effectiveness and ease of use.

ACKNOWLEDGEMENTS

The authors acknowledge funding support by the DARPA VAPR program. All device fabrication was done at the Cornell NanoScale Facility (CNF), a member of the National Nanotechnology Infrastructure Network.

REFERENCES

[1] I. Blakey, *et al.*, "Polycarbonate based nonchemically amplified photoresists for extreme ultraviolet lithography," *Proceedings of SPIE*, Vol. 7636, 2010.

[2] Legrand and Bendler, *Handbook of Polycarbonate Science and Technology*, Marcel Dekker, 1999.

[3] F. M. Houlihan, *et al.*, "Thermally Depolymerizable Polycarbonates. 2. Synthesis of Novel Linear Tertiary Copolycarbonates by Phase-Transfer Catalysis", *Macromolecules*, pp13-19, 1986.

[4] Berger, *et al.*, "Micromechanical thermogravimetry," *Chemical Physics Letters*, 1989.

[5] Semancik, *et al.*, "Microhotplate platforms for chemical sensor research," *Sensors and Actuators B: Chemical*, pp. 579-591, 2001.

[6] V. Kaajakari and A. Lal, "Ultrasonically driven surface micromachined motor," *Proc. of 13th IEEE International Conference on Micro Electro Mechanical Systems*, 2000.

[7] K. S. Novoselov, *et al.*, "Electric Field Effect in Atomically Thin Carbon Films," *Science*, Vol 306, pp. 666-669, 2004.

[8] V. Georgakilas, *et al.*, "Functionalization of Graphene: Covalent and Non-Covalent Approaches, Derivatives and Applications," *Chemical Reviews*, 2009.

[9] Graff, *Wave Motion in Elastic Solids*, Dover, 1991.

[10] H. Hosseinzadegan and A. Lal, "Tip-based graphene etching for MEMS resonator frequency trimming", in *Tech. Digest of the 17th International Conference on Solid-State Sensors, Actuators and Microsystems (Transducers '13)*, 2013.

[11] J. M. Frechet *et al.*, "Thermally Depolymerizable Polycarbonates V. Acid Catalyzed Thermolysis of Allylic and Benzylic Polycarbonates: A new Route to Resist Imaging", *Polymer Journal*, 1987.

[12] J. Moser, *et al.*, "Current-induced cleaning of graphene", *Applied Physics Letters,* 2007.

CONTACT

*V. Gund, tel: +1-650-521-1172; vvg3@cornell.edu